

IDENTIFICATION AND CLASSIFICATION OF MIXED PHYTOPLANKTON ASSEMBLAGES USING AVIRIS IMAGE-DERIVED SPECTRA

Laurie L. Richardson
Department of Biological Sciences
Florida International University
Miami, Florida 33199 USA
richardl@fiu.edu

and

Fred A. Kruse
Analytical Imaging and Geophysics LLC
4450 Arapahoe Ave, Suite 100
Boulder, Colorado 80303 USA
kruse@aigllc.com

1. INTRODUCTION

The enormous potential for using hyperspectral imaging sensor data to study the Earth's surface has been known for several years (Goetz et al., 1985). This potential is largely based on the capability of such sensors to provide high resolution spectra, on a per pixel basis, along with image data. This capability is of direct importance in that many features of the Earth's surface have distinctive spectral reflectance signatures. Hyperspectral sensors can take advantage of this planetary trait by enabling the extraction of spectral information from Earth surface features on a regional scale. Highly successful results have been obtained following this approach, particularly in the field of geology where exposed lithographies have been mapped based on specific mineral spectral reflectance signatures (Boardman et al, 1995; Kruse et al, 1996).

We are applying an approach similar to that being used by geologists to the study of aquatic ecosystems, in particular those that have high concentrations of phytoplankton. It has been known for many years that different types of phytoplankton contain different, taxonomically significant accessory pigments (Rowan, 1989). It is also well known that each algal pigment is spectrally unique (Morton, 1975). As a result, the (spectral absorbance based) detection of taxonomically specific pigment signatures is being used to reveal the types of algae (phytoplankton) present in different aquatic ecosystems, which in turn yields information such as trophic status (Gieskes, 1991). A parallel approach, targeting analysis of algal pigment reflectance spectra (as opposed to absorbance spectra), has been carried out for AVIRIS both on a theoretical basis (Dekker and Hoogenboom, 1996) and with AVIRIS data acquired over aquatic systems (Richardson et al, 1994; Richardson, 1996; Richardson and Ambrosia, 1996). Success by both groups has been obtained in detecting algal pigment signatures using AVIRIS spectra, resulting in the identification of the types of phytoplankton present.

The use of AVIRIS data for identifying spectral signatures of Earth surface features can be extended in that the spectral information derived from AVIRIS imagery (analyzed, for example, to identify specific minerals or phytoplankton pigments) can be further used to classify AVIRIS image data (Goetz, 1985). Again, highly successful results have been obtained in geological applications using this approach (Boardman et al, 1995). We report here our recent results in applying these procedures to identify, classify, and map phytoplankton blooms with different algal compositions in Florida Bay using AVIRIS image-derived spectra. Our overall approach of applying techniques developed for geological analysis of AVIRIS data to analysis of phytoplankton in aquatic ecosystems has

been published previously (Kruse et al., 1997).

2. METHODS

2.1 Field Site

Florida Bay is a shallow (<2 m), estuarine ecosystem located south of the Florida peninsula and to the east and north of the Florida Keys. The bay consists of numerous sub-basins, separated by shallow water several cm deep or areas of exposed sediment. Since the early 1990's the bay has exhibited annual phytoplankton blooms resulting in optically dense (highly colored) water. These blooms consist of phytoplankton of three major groups: diatoms, cyanobacteria ("bluegreen algae") and microscopic green algae. Blooms may be unialgal or mixed, and concentrated to varying degrees. We have been studying the bay as a natural laboratory to investigate remote sensing of algal accessory pigments for a number of years. The ecosystem, in the context of use as a field site for our hyperspectral work, has been described previously (Richardson et al, 1995; Richardson and Ambrosia, 1997). These earlier publications include phytoplankton pigment data and spectroradiometer data we have collected for several years as background data to support our AVIRIS research.

2.2 AVIRIS Data and Groundtruthing

AVIRIS data of Florida Bay were acquired on 3/23/96. The AVIRIS sensor was flown on NASA's ER-2 high-altitude aircraft, which provided a pixel size of 20 m per side (low spatial resolution mode). Three flight runs across the bay yielded a total of 11 scenes, each of which imaged an area 10 x 12 km. Groundtruth measurements were performed from a small boat on the same day, with data acquired between 11:00 and 14:30 (Eastern standard time). Data were obtained from seven basins within the bay, and consisted of water samples (for laboratory based phytoplankton pigment analysis), spectroradiometer (Spectron Engineering SE590) measurements of water surface reflectance and a spectralon calibration panel, GPS coordinates of each sample site, and visual observations.

2.3 Pigment Data

Phytoplankton pigments were extracted from filtered water samples and analyzed using High Performance Liquid Chromatography (HPLC). Both the methodology used and the results of analysis of the 3/23/96 data set have been published previously (Richardson and Ambrosia, 1997).

2.4 AVIRIS Data Processing

AVIRIS data were first atmospherically corrected using ATREM (the Atmospheric Removal Program). Further processing was carried out using ENVI (the Environment for Visualizing Imagery) software. As an initial step, a spectral library was generated by extracting end-member spectra from the imagery. End-member spectra were derived from pixels that corresponded to sampling stations during the AVIRIS flight. Pixels were located on the image using GPS information obtained during sampling, and maps of Florida Bay.

AVIRIS spectra utilized to build the spectral library were derived from a spectral subset of the AVIRIS data. The spectral subset consisted of 60 bands (bands 1 through 60) with two bands (32 and 33) removed. [These bands were removed because they cover the area of the A/B spectrometer overlap.] Thus a total of 58 bands were used. Band centers were located between 370-930 nm, which covers the visible and near infrared areas of the electromagnetic spectrum. It is this area where pigment-related phytoplankton reflectance signatures are present.

The data presented in this paper are from 1 AVIRIS scene (run 8 scene 10). Four of the seven ground-truth stations are imaged on this one scene. Prior to classification this scene was subsampled in the same manner as during generation of the spectral library so that only bands 1 through 60 (with bands 32 and 33 removed) were used.

The spectrally subsampled, but full scene, image was classified (using the image-derived endmembers in the spectral library) using the Spectral Angle Mapper (SAM) algorithm available in ENVI. As user input to the program, a maximum spectral angle of 0.05 radians, or 0.10 radians, was used. Image processing methods have been described in detail previously (Kruse et al, 1993, 1997).

3. RESULTS AND DISCUSSION

The locations of the four sampling (groundtruth) stations imaged in run 8 scene 10 are shown (annotated on the imagery) in Figure 1. Each station was located within a sub-basin of Florida Bay, and was named based on a nearby key (small mangrove island). In the image, the dark areas correspond to exposed sediment, often present between basins. Groundtruth stations were located on the imagery using GPS-acquired latitude/longitude coordinates and maps.

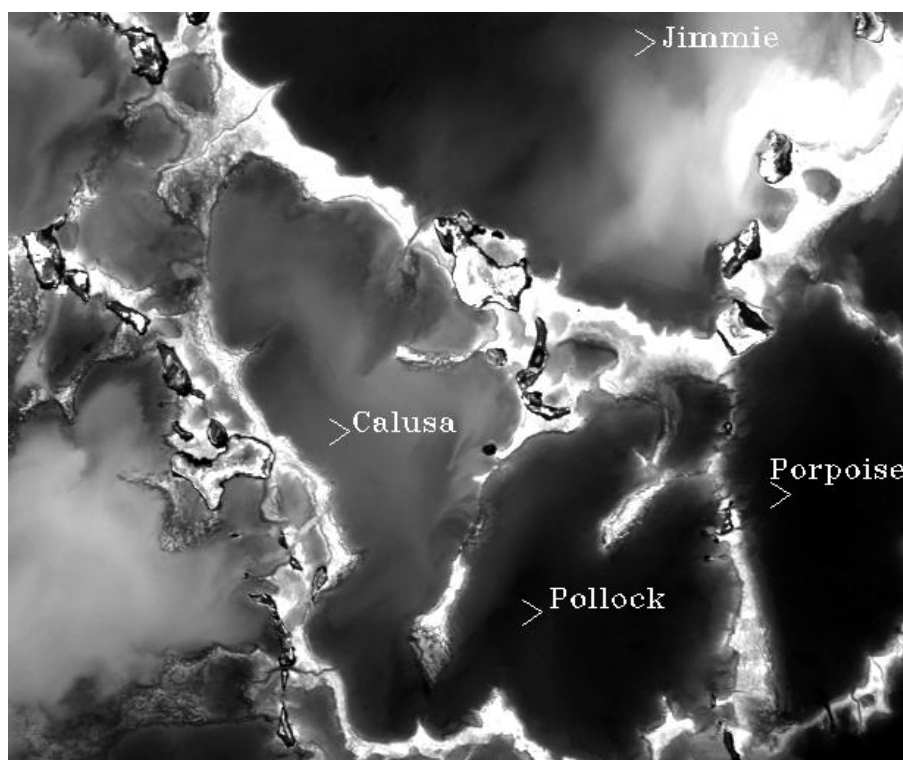


Figure 1. AVIRIS image with groundtruth (sampling) stations in four sub-basins of Florida Bay indicated by arrows.

Pigment data for samples collected at each of the four stations are summarized in Table 1. The pigment data presented (4 pigments) are a subset of the total pigment data analyzed. The complete pigment data set, which includes 9 pigments analyzed at each of 7 stations, has been published previously (Richardson and Ambrosia, 1997). For this paper, the 4 pigments presented in Table 1 were selected as indicator pigments to discriminate between the three major phytoplankton types that were present: diatoms, cyanobacteria, and green algae. While all algae (including phytoplankton) have chlorophyll *a* (the photosynthetic reaction center pigment), chlorophyll *b* is indicative of green algae, and chlorophyll *c* of diatoms. One carotenoid pigment, myxoxanthophyll, is also presented. This pigment is specific to cyanobacteria. Thus on 3/23/96 the four basins can be seen to have four different bloom compositions: diatoms only (Calusa); diatoms and

cyanobacteria (Pollock and Porpoise); and diatoms, cyanobacteria and green algae (Jimmie). While both Pollock and Porpoise had a bloom composition with the same two major phytoplankton groups (cyanobacteria and diatoms), they were present in different proportions. This can be seen by considering pigment ratios. Thus Pollock has a myxoxanthophyll to chlorophyll *a* ratio of 1:7, whereas Porpoise has a corresponding ratio of 1:6. The chlorophyll *c* to chlorophyll *a* ratios in the two basins are the same, revealing that cyanobacteria constitute a relatively larger proportion of the mixed bloom in Porpoise when compared to Pollock. The relative concentration of chlorophyll *a* is useful to indicate relative abundance of phytoplankton, and is commonly the only pigment analyzed to estimate phytoplankton biomass. As seen in Table 1, Jimmie had the most dense bloom. When considering taxonomically significant accessory pigments, chlorophyll *a* is also useful for pigment ratios to assess the relative abundance of different types of phytoplankton.

Table 1. Algal Accessory Pigments ($\mu\text{g/l}$) in Basins During the AVIRIS Flight

<u>Pigments</u>	<u>Calusa</u>	<u>Jimmie</u>	<u>Pollock</u>	<u>Porpoise</u>
chlorophyll <i>a</i>	0.39 $\mu\text{g/l}$	0.80 $\mu\text{g/l}$	0.42 $\mu\text{g/l}$	0.36 $\mu\text{g/l}$
chlorophyll <i>b</i>	0	0.13 $\mu\text{g/l}$	0	0
chlorophyll <i>c</i>	0.14 $\mu\text{g/l}$	0.13 $\mu\text{g/l}$	0.14 $\mu\text{g/l}$	0.12 $\mu\text{g/l}$
myxoxanthophyll	0	0.08 $\mu\text{g/l}$	0.06 $\mu\text{g/l}$	0.06 $\mu\text{g/l}$

Figure 2 shows the four endmember spectra extracted from AVIRIS image pixels that corresponded to the sample stations depicted in Figure 1. These stations had different blooms of phytoplankton present as discussed above. The spectra are shown in terms of band number instead of wavelength. Bands 1 to 60 were

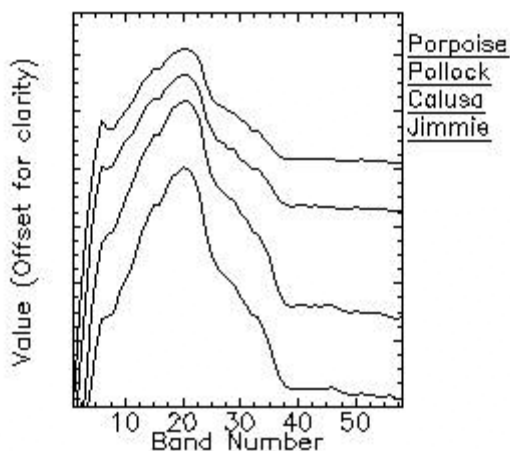
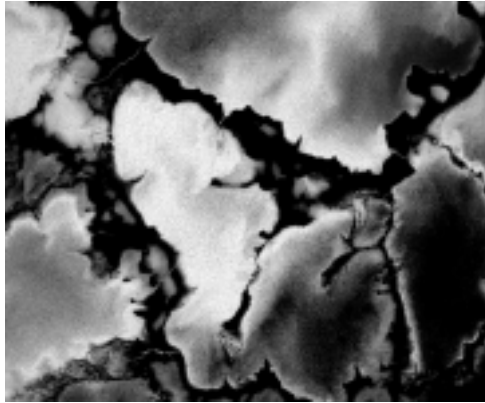
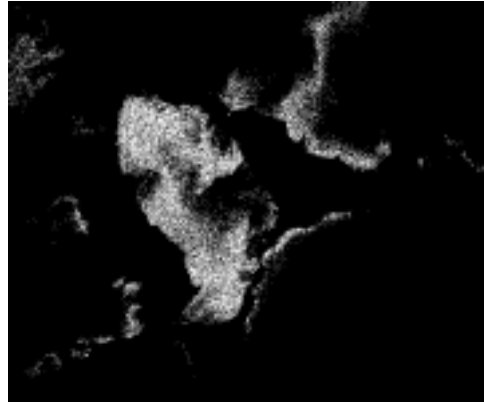


Figure 2. Endmember spectra used for image classification.



A1



A2



B1



B2

Figure 3. Rule images (left) and classification outputs (right) produced using the SAM algorithm.
Plates A1 and A2 = Calusa. Plates B1 and B2 = Jimmie.

used, which correspond to a wavelength range from ca. 365 to 935 nm (band centers at 370 and 930 nm). The overall shapes of these spectra are similar, revealing the dominant green reflectance of chlorophyll *a*. Detection of accessory pigment signals within these spectra requires use of fourth derivative spectral analysis (see Richardson and Ambrosia, 1996; Dekker and Hoogenboom, 1996). In very highly colored waters the accessory pigment features are evident in the AVIRIS image-derived spectra themselves (Richardson et al, 1994).

The spectral library shown in Figure 2 was used to classify the (spectrally subsampled) full scene. Results are presented in Figures 3 and 4. The Spectral Angle Mapper (SAM) algorithm was selected for the classification process because of our interest in spectral signatures. This algorithm computes the spectral similarity between an end-member spectrum and each spectrum in the image. During the calculation, rule



C1



C2



D1



D2

Figure 3, cont. Rule images (left) and classification outputs (right) produced using the SAM algorithm.
Plates C1 and C2 = Pollock. Plates D1 and D2 = Porpoise.

images are generated that depict the calculated distance between the endmember spectrum and each pixel spectrum on a gray scale. As depicted in Figure 3 (images on the left of each pair), lighter pixels represent closer spectral matches. The classification outputs are also depicted in Figure 3 (images on the right of each pair). For the classification images, only those pixels classified to have a spectral angle of less than 0.05 radians were classified (black pixels). For the classification images, unclassified pixels are presented as white. The distributions of the four different phytoplankton blooms among the subbasins is apparent. In one case (see Figure 3D2), image pixels were classified only in the groundtruth basin (Porpoise) and an adjacent basin (Pollock). This bloom was composed of diatoms and cyanobacteria, with relatively more cyanobacteria than Pollock, which contained the same two types of phytoplankton. Image pixels classified as corresponding to the Pollock bloom were found in four basins (Figure

3C2). The unialgal diatom bloom occurred in basins throughout out the scene (Figure 3A2), especially near the edges of basins. The latter observation is interesting in an ecological sense in that diatoms are relatively more tolerant of high light (as would be found in shallow water). The mixed bloom (diatoms, cyanobacteria and green algae) found in Jimmie was concentrated both in the eastern side of that basin and, to lesser extents, in Calusa.

Figure 4 shows a classification in which the scene was classified using all four endmember spectra. While most of the basins were classified as one of the four phytoplankton bloom types, the water in some subbasins remained unclassified (see, for example, the basin to the left of Calusa). The identity of phytoplankton within these areas is not known at this time. The image of Figure 4 utilized a SAM maximum spectral angle of 0.10 radians, as opposed to the maximum angle of 0.05 used in the classifications presented in Figure 3. Results using the larger spectral angle are presented here because they classify most of the basins within the scene. Our future efforts include incorporation of a spectroradiometer ground truth data set (see Richardson et al, 1995) consisting of monthly measurements supported by pigment, and in some cases, phytoplankton cell count data, acquired throughout Florida Bay from 1994 through 1996. We anticipate that use of these data will classify the unclassified basins mentioned above, and allow use of a smaller spectral angle maximum to classify all basins.

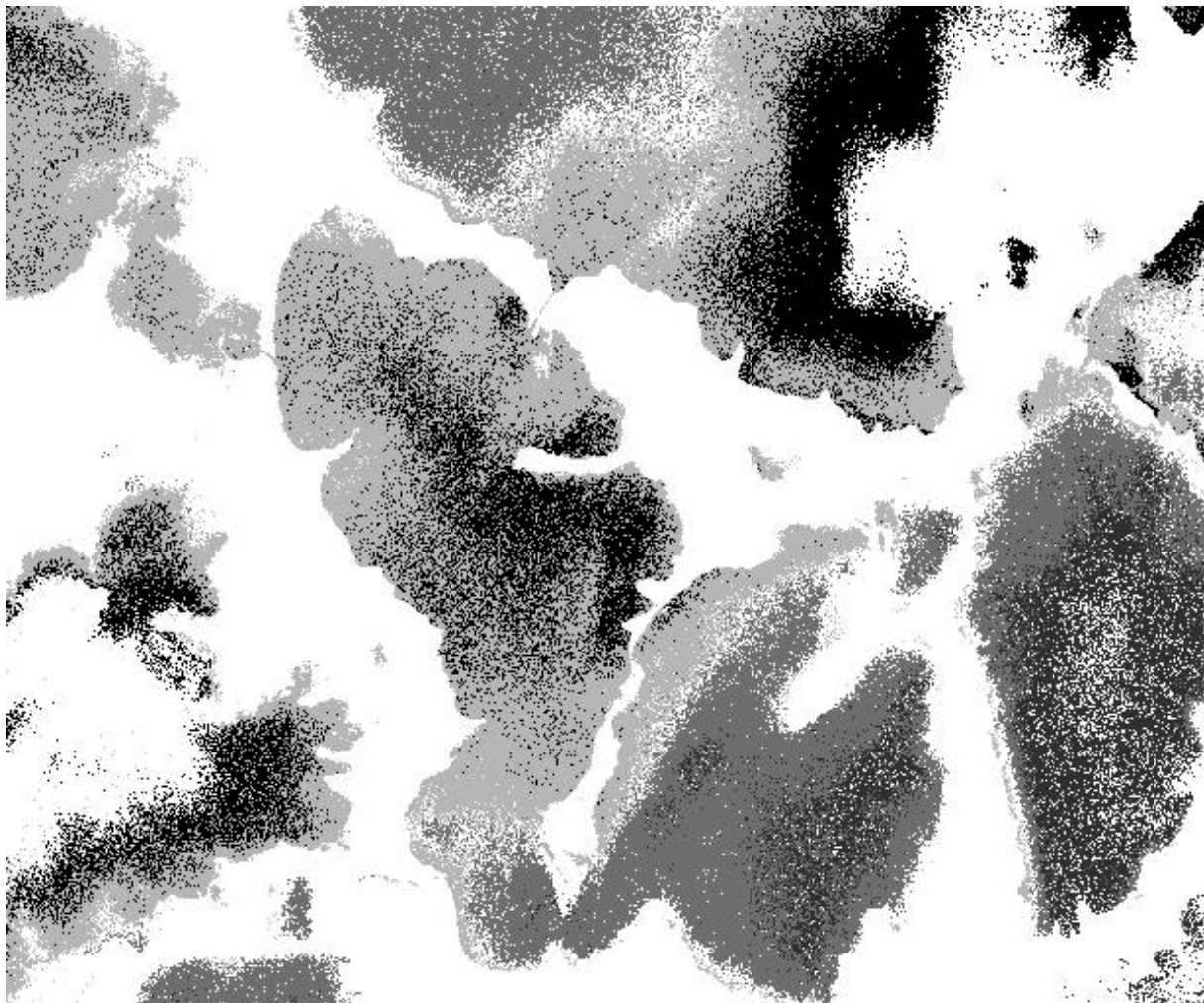


Figure 4. SAM classification using the four endmember spectra. Light grey = Calusa; medium grey = Pollock; dark grey = Porpoise; black = Jimmie. (unclassified = white)

4. CONCLUSIONS

Our results indicate that AVIRIS data of an aquatic ecosystem (Florida Bay) can be classified as to phytoplankton composition using AVIRIS image-derived spectra. The endmember spectra we used were extracted from AVIRIS image pixels in basins that were groundtruthed, thus contained known phytoplankton assemblages. Based on earlier results by ourselves (and others) we are interpreting our success as based on the differences in spectral signatures due to algal accessory pigments. This conclusion stems from the spectral basis of the algorithm used for the classification (the Spectral Angle Mapper) and the fact that the optical signature of such phytoplankton-rich waters is dominated by pigments. Using this approach we were able to discriminate and classify three phytoplankton bloom types: diatoms (unialgal), diatoms and cyanobacteria, and a mixed population of diatoms, cyanobacteria and green microalgae. Additionally, two populations with the same phytoplankton composition but different amounts of two phytoplankton types were separable.

At this point we are focusing on detecting different phytoplankton bloom compositions using spectral matching techniques. Future efforts aimed at quantifying the biomass of different phytoplankton populations within blooms will require more refined classifying approaches, which in turn will require new development of algorithms for non-linear mixing (discussed in Kruse et al, 1997). We anticipate that while this approach is successful in phytoplankton-rich coastal waters, results will be less than satisfactory in relatively phytoplankton-poor, offshore waters. In such waters the phytoplankton pigment signatures are obscured by the absorption of water itself unless phytoplankton blooms are present at the surface.

5. ACKNOWLEDGMENTS This research is supported by NASA (grants NAG5-3124 and NAG5-8156).

6. REFERENCES

- Boardman, J.W., F.A. Kruse and R.O. Green, 1995, "Mapping Target Signatures Via Partial Unmixing of AVIRIS Data", Summ. 5th Ann. JPL Airborne Earth Sci. Workshop, JPL Pub. 95-1, vol. 1, pp. 23-26.
- Dekker, A.G. and H.J. Hoogenboom, 1996, "Predictive Modelling of AVIRIS Performance Over Inland Waters", Summ. 6th Ann. JPL Airborne Earth Sci. Workshop, JPL Pub. 96-4, vol. 1, pp. 83-92.
- Gieskes, W.W., 1991, "Algal Pigment Fingerprints: Clue to Taxon Specific Abundance, Productivity, and Degradation of Phytoplankton in Seas and Oceans," in S. Demers (ed.), Particle Analysis in Oceanography, NATO ASI Series, Springer-Verlag, Berlin, vol. G27, pp. 61-99.
- Goetz, A.F.H., G. Vane, J.E. Solomon and B.N. Rock, 1985, "Imaging Spectrometry for Earth Remote Sensing", Science, vol. 228, pp. 1147-1153.
- Kruse, F.A., A.G. Lefkoff, J.W. Boardman, K.B. Heidebrecht, A.T. Shapiro, P.J. Barloon, and A.F.H. Goetz, 1993, "The Spectral Image Processing System (SIPS) - Interactive Visualization and Analysis of Imaging Spectrometer Data", Rem. Sens. Env., vol. 44, pp. 145-163.
- Kruse, F.A., J.H. Huntington and R.O. Green, 1996, "Results from the 1995 AVIRIS Geology Group Shoot", Proc. 2nd Intl. Airborne Rem. Sens. Conf. Exh., ERIM, vol. 1, pp. 211-220.
- Kruse, F.A., L.L. Richardson and V.G. Ambrosia, 1997, "Techniques Developed for Geologic Analysis of Hyperspectral Data Applied to Near-Shore Hyperspectral Ocean Data", Proc. 4th Intl. Conf. Rem. Sens. Mar. Coast. Env., ERIM, vol. I, pp. 233-246.
- Morton, A.M., 1975, "Biochemical Spectroscopy", Wiley and Sons, N.Y., Vol. 1.
- Richardson, L.L., 1996, "Remote Sensing of Algal Bloom Dynamics", BioScience, vol. 46, pp. 492-501.

Richardson, L.L., D. Buisson, C.J. Liu and V. Ambrosia, 1994, "The Detection of Algal Photosynthetic Accessory Pigments Using Airborne Visible-Infrared Imaging Spectrometer (AVIRIS) Spectral Data," Mar. Tech. Soc. J., vol. 3, pp.10-21.

Richardson, L.L., D. Buisson and V. Ambrosia, 1995, "Use of Remote Sensing Coupled with Algal Accessory Pigment Data to Study Phytoplankton Bloom Dynamics in Florida Bay," Proc. 3rd Them. Conf. Rem. Sens. Mar. Coast. Env., ERIM, vol. I, pp. 183-192.

Richardson, L.L. and V.G. Ambrosia, 1996, "Algal Accessory Pigment Detection Using AVIRIS Image-Derived Spectral Radiance Data", Summ. 6th Ann. JPL Airborne Earth Sci. Workshop, JPL Pub. 96-4, vol. 1, pp. 189-196.

Richardson, L.L. and V.G. Ambrosia, 1997, "Remote Sensing of Algal Pigments to Determine Coastal Phytoplankton Dynamics in Florida Bay," Proc. 4th Intl. Conf. Rem. Sens. Mar. Coast. Env., vol. I, pp. 75-81.

Rowan, K.S., 1989, "Photosynthetic Pigments of Algae", Cambridge University Press, Cambridge.